Published in final edited form as:
FEMS Microbiol Ecol. 2013 May ; 84(2): 344–354. doi:10.1111/1574-6941.12066.

Effects of fluid flow conditions on interactions between species in biofilms

Wei Zhang[1], **Tadas Sileika**[1], and **Aaron I. Packman**[1,*]

[1]Department of Civil and Environmental Engineering, Northwestern University, Evanston, IL, 60208

Abstract

Most microbes live in complex communities, where they interact both synergistically and competitively. In order to explore the relationship between environmental heterogeneity and the spatial structure of well-defined biofilms, single- and mixed-species biofilms of *Pseudomonas aeruginosa* PAO1 and *Flavobacterium sp.* CDC-65 were grown in a planar flow cell under highly controlled flow gradients. Both organisms behaved differently in mixed cultures than in single-species cultures due to inter-species interactions, and these interactions were significantly affected by external flow conditions. *Pseudomonas* and *Flavobacterium* showed a competitive relationship under slow inflow conditions, where the supply of growth medium was limited. Under such competitive conditions, the faster specific growth rate of *Flavobacterium* allowed it to secure access to favorable regions of the biofilm by over-growing *Pseudomonas*. In contrast, *Pseudomonas* was restricted to nutritionally depleted habitat near the base of the biofilm, and its growth was significantly inhibited. Conversely, under higher inflow conditions providing greater influx of growth medium, both organisms accumulated greater biomass in mixed biofilms than in single-species biofilms. Spatial segregation of the two organisms within the biofilms contributed to enhanced overall exploitation of available nutrients and substrates, while morphological changes favored better adherence to the surface under high hydrodynamic shear. These results indicate that synergy and competition in biofilms varies with flow conditions. Limited resource replenishment favors competition under low-flow conditions, while high flow reduces competition and favors synergy by providing greater resources and simultaneously imposing increased hydrodynamic shear that makes it more difficult to accumulate biomass on the surface. Ecological interactions that produce mechanically stronger and more robust biofilms will support more extensive growth on surfaces subject to high hydrodynamic shear, but these interactions are difficult to predict from observations of the behavior of individual organisms.

Keywords

dual-species biofilm; multi-species interaction; flow gradients; *Pseudomonas aeruginosa*; *Flavobacterium*

1 Introduction

Culture-based and non-culture approaches have revealed that microorganisms rarely live alone, but rather interact with each other to form complex communities. Although some microbial communities consist of free-swimming cells in aquatic environments, most microbial communities grow on interfaces as biofilms (Ward*, et al.*, 1998, Davey & O'toole,

*Corresponding author: Aaron I. Packman, 2145 Sheridan Road, Evanston, IL 60208-3109, A314 Technological Institute, Phone: (847) 491-9902, Fax: (847) 491-4011, a-packman@northwestern.edu.

2000, Kolenbrander, 2000, Zengler, 2009). Organisms in biofilms are involved in both symbiosis and competition for resources, and these interactions are affected by organism distributions, biofilm structures, and spatial heterogeneity. Well-defined multi-species biofilms have been used as simplified model systems in microbial ecology to follow community development, identify the role of individual populations in the community, and observe responses of microbial communities to environmental gradients. Such interactions have been observed in layered sludge granules, organized phototrophic consortia, and colonization of biofilms by planktonic organisms (Sekiguchi, *et al.*, 1999, Overmann & van Gemerden, 2000, An, *et al.*, 2006, Hansen, *et al.*, 2007, Beaufort, *et al.*, 2012).

Pseudomonas aeruginosa and *Flavobacterium spp.* are two of the most ubiquitous opportunistic pathogens found in rivers, lakes, and engineered water systems (Ford, 1999, Manz, *et al.*, 1999, Brinkmeyer, *et al.*, 2003). They are major sources of nosocomial pneumonias and bacteremia from hospital devices and water supply systems, and they have been found to be major contributors of biofilms associated with outbreaks of Legionellosis (Stamm, *et al.*, 1975, Orrison, *et al.*, 1983, Pearson, *et al.*, 1996, Anaissie, *et al.*, 2002). These two organisms have previously been used to form a well-defined consortium with *Klebsiella pneumoniae* to examine the survival and growth of *Legionella pneumophila* in biofilms (Murga, *et al.*, 2001), and to study biofilm colonization and disinfection in pilot-scale cooling tower systems (Liu, *et al.*, 2009, Liu, *et al.*, 2011). *P. aeruginosa* has been observed to dominate the community in closed batch systems while *Flavobacterium* has been found to dominate in open (flow-through) systems (Liu, *et al.*, 2009). However, the specific environmental conditions responsible for this behavior are still unclear. Many studies have indicated that the development and morphology of biofilms is significantly affected by external hydrodynamic forces, inputs and outputs of nutrients and substrates, and chemical transport. Replenishment of nutrients and substrates (such as carbon sources, nitrogen sources and oxygen) is essential for biofilm growth, and this replenishment increases with flow rate, but the accompanying hydrodynamic forces also affect biofilm structure and can lead to detachment from the substratum (Chopp, *et al.*, 2002, Liu & Tay, 2002, Purevdorj, *et al.*, 2002, Battin, *et al.*, 2003).

Here the behavior of a model ecosystem composed of *Pseudomonas aeruginosa* PAO1 and *Flavobacterium sp.* CDC-65 was examined under well-defined environmental gradients in a planar flow cell. The flow cell system allowed biofilm growth to be monitored non-invasively for seven days under imposed gradients of local velocity, hydrodynamic shear stress, and influx of growth medium. We hypothesized that patterns of biofilm growth would be directly related to the imposed environmental heterogeneity, and that each organism would colonize regions of the biofilm where local conditions particularly favored its growth.

2 Methods and Materials

2.1 Bacteria strains and propagation

Pseudomonas aeruginosa strain PAO1 with chromosomally encoded green fluorescent protein (GFP) and *Flavobacterium sp.* CDC-65 were used in flow-cells experiments (Orrison, *et al.*, 1983, Stover, *et al.*, 2000, Murga, *et al.*, 2001). R2A medium was used to simulate typical depleted environmental water conditions. R2A medium contained (per liter): 0.05 g of yeast extract, 0.05 g of proteose peptone No. 3, 0.05 g of casamino acids, 0.05 g of dextrose, 0.03 g of sodium pyruvate, 0.03 g of dipotassium phosphate, and 0.005 g of magnesium sulfate (Murga, *et al.*, 2001). Stock cultures of *Pseudomonas* and *Flavobacterium* were streaked onto R2A agar plates and incubated at 30°C for 24 hours. R2Aagar was R2A medium with the addition of 15 g per liter agar. A single colony of each strain was transferred into 5 ml of R2A medium, and grown at 30°C with shaking to

stationary phase. Each culture was then transferred to fresh medium and diluted to OD_{600} = 0.1 for inoculation into the flow cell.

Flow cell experiments were conducted at room temperature, 25°C. In order to help interpret the relative growth of the two organisms in flow cells, the growth curve of each strain in R2A liquid medium was measured at 25°C in triplicate. Specific growth rates at exponential phase of each organism were then calculated from these results (Elvers*, et al.*, 1998). To confirm that metabolic products of each organism didn't inhibit the other organism's growth, disk sensitivity tests were performed using suspensions of each species following the methods of Nikoskelainen *et al.* (Nikoskelainen*, et al.*, 2001).

2.2 Flow cell experiments

We cultivated biofilms in the planar flow cell system described in Zhang *et al.* (Zhang*, et al.*, 2011) to support biofilm growth under essentially two-dimensional flow conditions. The flow cell chamber has dimensions of 3.5 cm × 3.5 cm × 0.06 cm. The flow configuration is shown in Figure 1A, and detailed descriptions of the geometry and performance of this flow cell is available in Zhang et al. (2011). Biofilms were grown under the right-angle flow pattern shown in Figure 1B. This flow configuration produces distinct gradients of hydrodynamic shear and influx of growth medium from the bottom-right to the upper-left of the flow chamber. Biofilm growth was observed in the center region of the flow cell where there is a regular flow gradient, as shown in Figure 1C. Results are presented for each of the nine observation locations denoted R1 to R9 in Figure 1C. The lattice Boltzmann method was used to simulate the flow field throughout the flow cell and solute transport from inlets to observation regions (Zhang*, et al.*, 2011).

Flow cell experiments were performed with both single-species cultures of *Pseudomonas* and *Flavobacterium* and mixed-species cultures of the two organisms. In the multi-species experiments, separate batch cultures of *Pseudomonas* and *Flavobacterium* were grown to the stationary phase, and then inoculated at a ratio of 1:1 into flow cells. After inoculation, the flow cell was inverted for one hour to facilitate adherence of cells to the glass cover slip, and then returned back to the original position. Microscopic observations confirmed that this procedure evenly distributed *Pseudomonas* and *Flavobacterium* on the substratum (results not shown). Then R2A media was introduced by means of a peristaltic pump (Gilson Mini Plus3) particularly suitable for biofilm experiments because it has minimal flow pulsation. Flow cell experiments were performed under two flow rates, a slower inflow rate of 0.16 mL min^{-1} and a faster inflow rate of 0.80 mL min^{-1}, in duplicate. We chose these conditions because we previously observed that they produced distinct patterns of growth and detachment in *P. aeruginosa* biofilms (Zhang, et al., 2011). The slow inflow rate provided a velocity gradient from 2.52 cm min^{-1} in R1 to 3.72 cm min^{-1} in R9 in the observation window spanning the nine regions R1 to R9 shown in Figure 2A. The fast inflow rate provided velocities ranging from 5.76 cm min^{-1} in R1 to 10.4 cm min^{-1} in R9, as shown in Figure 2B.

2.3 Characterizing biofilm morphologies

A LSM 510 META confocal laser scanning microscope (Carl Zeiss) with a Plan-Apochromat 63×/1.4 NA oil immersion objective lens was used to image the biofilms. Three image stacks were collected in each region shown in Figure 1C. *Pseudomonas* was detected by its constitutively expressed green fluorescent protein (GFP). *Flavobacterium* was detected by counterstaining with nucleic acid dye, SYTO-62 (Molecular Probes). 50 μM of SYTO-62 was added into the flow cell and allowed to bind under stagnant conditions for 20 min in the dark, and then flow was resumed to rinse unbound dye. GFP and SYTO-62 was imaged using CLSM at excitation wavelengths of 488 nm and 633 nm, respectively. The

VOLOCITY software package (Improvision Inc.) was used to generate three-dimensional images from stacks of CLSM images, and the COMSTAT software was used for quantitative analysis of these three-dimensional images (Heydorn, *et al.*, 2000, Heydorn, *et al.*, 2000).

2.4 Statistical analysis

The one-factor t-test was used to assess differences in the biofilm structural characteristics associated with local velocity and solute travel time. Two-way analysis of variance was used to evaluate the changes in morphology of single- and multi-species biofilms under different flow conditions.

3 Results

3.1 Mixed-species biofilms under flow gradients

After 5 days of growth, the system reached a steady state in which the overall pattern of biofilm morphology and the distribution of the two species within the biofilm no longer changed with time. Figure 2 shows the biofilm morphology and spatial distributions of each organism within seven-day-old mixed-species biofilms.

Under slow inflow conditions, thin biofilms composed of both *Pseudomonas* and *Flavobacterium* were detected in all regions. *Pseudomonas* was present as sporadic small colonies and single cells, while *Flavobacterium* formed relatively continuous biofilms with larger clusters (Figure 2A). Regions R1, R2 and R4 had thinner *Flavobacterium* biofilms and more *Pseudomonas* colonies. Vertical distributions, presented in Figure 2C, indicate that *Pseudomonas* mainly occurred at the base of mixed biofilms and was overgrown by *Flavobacterium*. In all regions, at all elevations, *Flavobacterium* was the dominant component of biomass in the seven-day biofilm.

Under fast inflow conditions, more complex intergrowth of the two organisms was observed. The biofilm morphologies and the vertical distributions of each organism are shown in Figure 2B and 2D, respectively. *Pseudomonas* always formed the base of mixed biofilms while *Flavobacterium* dominated the upper part of the biofilm canopy. In regions R1, R4 and R7, *Pseudomonas* occurred in a smooth, continuous, and thin base layer, while *Flavobacterium* formed discontinuous large tufts and clusters on top of *Pseudomonas* biofilms. In these regions, *Pseudomonas* was the dominant organism at the base of the biofilm: it represented over 50% of the biomass in the bottom 10 μm, and *Flavobacterium* was the dominant organism above 10 μm. The fraction of *Pseudomonas* gradually decreased until it was absent at a height of 27 μm in R1, and at 16 μm in R4 and R7. The maximum height of the *Flavobacterium* biofilm was 36 μm. In locations R2 and R5, *Flavobacterium* also existed as large tufts with pillars and towers of cells, while *Pseudomonas* occurred only in a thin and continuous layer at the base of the biofilm. In these regions, *Flavobacterium* reached maximum thicknesses of 50 μm at location R2 and 58 μm at location R5, while *Pseudomonas* disappeared at 19 μm (R2) and 15 μm (R5). Smoother biofilms formed in regions of faster local velocity. Region R8 had a faster velocity (9.78 cm min^{-1}), leading to greater accumulation of *Pseudomonas* and *Flavobacterium* and the formation of some tower structures. *Pseudomonas* was the dominant organism to a height of 18 μm and disappeared at 25 μm, while *Flavobacterium* was found at a maximum height of 44 μm. Regions R6 and R9 had the highest velocities (10.1 cm min^{-1} and 10.4 cm min^{-1}, respectively), and accumulated more *Pseudomonas* than other regions. *Pseudomonas* was the dominant organism to a height of 23 μm at R6 and 16 μm at R9, whereas *Flavobacterium* only achieved maximum heights of 36 μm at R6 and 29 μm at R9.

3.2 Single-species biofilms under flow gradients

We observed the behavior of single-species *Pseudomonas* and *Flavobacterium* biofilms to provide a basis for evaluating their interactions in mixed-species biofilms. Single-species *Pseudomonas* biofilms achieved steady state after four days and single-species *Flavobacterium* biofilms achieved steady state after six days. Figure 3 shows the morphologies of seven-day single-species biofilms of *Pseudomonas* and *Flavobacterium* under the two inflow rates.

Morphological gradients were observed in single-species *Pseudomonas* biofilms relative to the imposed flow gradient. *Pseudomonas* formed sporadic small colonies under the slower inflow condition. When the local velocity increased from 2.52 cm min^{-1} to 3.72 cm min^{-1}, the number of colonies increased with local flow velocity, but there was no continuous biofilm detected under these conditions (Figure 3A). More continuous biofilms formed under the faster inflow condition (Figure 3C). Large clusters formed in region R1, where the local velocity was 5.76 cm min^{-1}. In regions R2 and R4, which had higher velocities of 7.62 cm min^{-1} and 7.50 cm min^{-1}, respectively, clusters connected together leading to higher surface coverage. Smooth, continuous biofilms developed in region R7, where the local velocity was 9.00 cm min^{-1}. Additional roughness developed under higher velocities at R5 and R3, and then more clusters, towers and mushroom features appeared under the fastest velocities in regions R6, R8, and R9.

Single-species *Flavobacterium* biofilms developed different morphologies under the same flow conditions. Under the slow inflow rate, very thin and discontinuous biofilms formed, and there was no significant difference between regions R1-R9, as shown in Figure 3B. Loose and filamentous biofilms formed under the fast inflow rate, and biofilm structures changed with local velocities as shown in Figure 3D. Sparse biofilms formed in region R1 under the flow velocity 5.76 cm min^{-1}. Rougher and thicker biofilms formed in regions R2, R3, R4, R5, and R7, which had higher velocities ranging from 7.50 cm min^{-1} to 9.36 cm min^{-1}. When the local velocity exceeded 9.78 cm min^{-1}, biofilms became looser and were unable to fully cover the substratum (regions R6, R8, and R9).

3.3 Quantitative description of biofilm morphology

Quantitative analysis of the confocal images supports more specific comparisons of differences in biofilm structure with flow conditions. We quantitatively compared the biofilm morphology using four parameters calculated from the confocal images: Biomass per unit area ($\mu m^3 \mu m^{-2}$), average biofilm thickness (μm), roughness (dimensionless), and surface-area-to-volume ratio (As/V, $\mu m^2 \mu m^{-3}$) (Heydorn, *et al.*, 2000).. These parameters are plotted as functions of local velocity in Figure 4.

Under velocities of 2.52–3.72 cm min^{-1}, *Flavobacterium* in mixed biofilms accumulated 0.4–0.9$\mu m^3 \mu m^{-2}$ biomass, while *Pseudomonas* biomass only reached 0.11–0.22 $\mu m^3 \mu m^{-2}$. Overall, *Flavobacterium* accumulated 4–7 times more biomass than *Pseudomonas*, and was the dominant member of the consortium in mixed biofilms ($p < 0.01$). The average thickness of the mixed biofilms increased from 0.34μm to 0.74μm under velocities of 2.52 cm min^{-1} to 3.24 cm min^{-1}, and then reached a constant value of 0.73 μm under velocities of 3.24–3.72 cm min^{-1}.

Under the fast flow conditions, the biomass of *Pseudomonas* in mixed cultures was around 7.0$\mu m^3 \mu m^{-2}$ under velocities of 7.50–9.00 cm min^{-1}, and rose above 10.0 $\mu m^3 \mu m^{-2}$ when velocity exceeded 9.36 cm min^{-1}. A positive relationship was observed between biomass accumulation and local velocity for *Flavobacterium* under low velocities, but this trend reversed under high local velocity. The *Flavobacterium* biomass increased from 3.8 $\mu m^3 \mu m^{-2}$ at 5.76 cm min^{-1} to 15.1 $\mu m^3 \mu m^{-2}$ at 9.78 cm min^{-1}, but declined to 12.6

$\mu m^3 \mu m^{-2}$ at 10.1 cm min^{-1} and even further to 9.2 $\mu m^3 \mu m^{-2}$ at 10.4 cm min^{-1} (R9). Total biomass showed the same trend as *Flavobacterium*, with a positive relationship between biomass accumulation and velocity until the velocity exceeded 9.78 cm min^{-1}. The average thickness of the mixed biofilms reached 38.9 μm under a velocity 9.78 cm min^{-1}, and then decreased with velocity to 32.7 μm under 10.1 cm min^{-1} and 26.5 μm under 10.4 cm min^{-1} (Figure 4B).

The roughness of mixed biofilms showed an inverse relationship with velocity under slow inflow conditions, with roughness decreasing from 1.0 to 0.7 as velocity increased from 2.52 cm min^{-1} to 3.72 cm min^{-1}. Under fast flow conditions, the roughness of mixed biofilms varied between 0.1 and 0.3 (Figure 4C). As/V values of mixed biofilms ranged from 1.5 to 2.8 $\mu m^2 \mu m^{-3}$ under velocities of 2.52–10.4 cm min^{-1}. In addition, mixed biofilms with more *Pseudomonas* biomass had less complex structures than those dominated by *Flavobacterium*. For instance, the lowest As/V observed in mixed biofilms, 1.5, occurred in locations R1 and R3 under velocities of 5.76 cm min^{-1} and 9.36 cm min^{-1}, where *Pseudomonas* had significantly greater biomass than Flavobacterium (Figure 4A).

To compare the difference between single-species biofilms and mixed-species biofilms, characteristics of single-species biofilms are shown in Figure 4. Under slow inflow conditions, biomass of both single-species biofilms showed a positive relationship with local velocity (inserts in Figures 4A and 4B). Single-species *Flavobacterium* biofilms had greater biomass (0.06–1.18 $\mu m^3 \mu m^{-2}$) than single-species *Pseudomonas* biofilms (biomass 0.03–0.46 $\mu m^3 \mu m^{-2}$). Compared with mixed biofilms, *Pseudomonas* accumulated more biomass in single-species cultures ($p < 0.01$), but *Flavobacterium* did not show a significant difference between mixed and single-species cultures ($p > 0.05$).

Under fast inflow conditions, single-species *Pseudomonas* biofilms showed a slight increase from 4.4 $\mu m^3 \mu m^{-2}$ to 7.5 $\mu m^3 \mu m^{-2}$ over the velocity range of 5.76–10.4 cm min^{-1}, and then maintained around 7.0 $\mu m^3 \mu m^{-2}$ of biomass up to a velocity of 10.4 cm min^{-1}. Single-species *Flavobacterium* biofilms accumulated less biomass than single-species *Pseudomonas*: 0.99 $\mu m^3 \mu m^{-2}$ under 5.76 cm min^{-1}, and 1.6–2.6 $\mu m^3 \mu m^{-2}$ at velocities from 7.50 cm min^{-1} to 10.4 cm min^{-1}. In addition, *Flavobacterium* accumulated significantly less biomass in single-species biofilms than it did in mixed biofilms ($p < 0.001$). Under higher local velocities, the average thickness of single-species *Pseudomonas* remained at 4.6–10.3 μm, while the thickness of single-species *Flavobacterium* increased slightly with velocity, though less than observed for single-species *Pseudomonas*. The single-species biofilms achieved significantly lower average thicknesses everywhere than mixed biofilms: single-species *Pseudomonas* biofilms were 2–4 times thinner and single-species *Flavobacterium* biofilms were 3–10 times thinner than the mixed-species biofilm (Figure 4B).

When local velocities increased from 2.52 cm min^{-1} to 3.72 cm min^{-1}, the roughness of both single-species biofilms declined: from 2.0 to 1.7 with *Pseudomonas* and from 2.0 to 1.6 with *Flavobacterium*. Similar behavior was observed in mixed biofilms, but single-species biofilms were rougher under all conditions. Under higher velocities, 5.76–10.4 cm min^{-1}, single-species *Pseudomonas* biofilms maintained a low roughness of 0.2–0.4, but *Flavobacterium* biofilms had a high roughness of 1.2–1.5 (Figure 4C).

In Figure 4D, it can be seen that As/V values of single-species *Pseudomonas* ranged between 2.0–3.1 $\mu m^2 \mu m^{-3}$ under slow inflow conditions, but single-species *Flavobacterium* had much greater As/V values of 5.0–8.2 $\mu m^2 \mu m^{-3}$. With the greater velocity under the fast inflow conditions, the As/V values of both organisms decreased. Single-species *Pseudomonas* biofilms had a small As/V of 0.5–1.5 $\mu m^2 \mu m^{-3}$ under velocities of 5.76–10.4

cm min^{-1}, and single-species *Flavobacterium* biofilms had As/V ranging from 3.7–4.8 $\mu m^2 \mu m^{-3}$. As/V values of mixed biofilms didn't significantly change from slow inflow conditions to fast inflow conditions. Moreover, they were similar with the values of single-species *Pseudomonas* biofilms under slow inflow conditions; while they were greater than that of single-species *Pseudomonas* biofilms and smaller than that of single-species *Flavobacterium* biofilms under fast inflow conditions.

3.4 Effects of solute transport on biofilm growth

Energy-yielding substrates and nutrients in growth media are consumed by metabolically active cells within biofilms. To test the effects of this depletion, we evaluated biofilm properties as a function of solute travel time and distance from the flow cell inlets. The travel distance to each location within the flow cell was calculated by integrating along the flow paths determined using the lattice Boltzmann model simulations, and the travel time was calculated similarly by integrating the local velocity along flow paths. Travel time and distance here are surrogate measures for the overall depletion of the growth medium during transport through the flow cell. We used these measures because we could calculate them directly for all locations in the flow cell, but we could not measure relevant chemical concentrations *in situ*. The solute travel time and distance from the flow cell inlets were calculated by the lattice Boltzmann simulations based on the velocity field shown in Figure 1B (Zhang*, et al.*, 2011).The relationship between biomass accumulation and solute travel time is shown in Figure 5, and the associated relationship with travel distance is presented in Supplementary Figure 1.

In single-species *Pseudomonas* biofilms, an inverse relationship was found between the solute travel time and biomass: when solute travel time increased from 0.6 min to 8.7 min, *Pseudomonas* biomass decreased from 7.5 $\mu m^3 \mu m^{-2}$ to 0.03 $\mu m^3 \mu m^{-2}$. A similar but weaker trend was found for *Pseudomonas* in mixed biofilms, with accumulated biomass decreasing from 12.2$\mu m^3 \mu m^{-2}$ at 0.6 min to 0.11$\mu m^3 \mu m^{-2}$ at 8.7 min. Single-species *Flavobacterium* biofilms accumulated biomass of 0.06–2.7 $\mu m^3 \mu m^{-2}$, but the amount of biomass did not decrease with solute travel time. *Flavobacterium* accumulated more biomass in mixed biofilms than in single-species culture, and interestingly, in mixed biofilms it also showed the inverse relationship between biomass and solute travel time as that observed for *Pseudomonas*. The biomass of *Flavobacterium* in mixed biofilms decreased from 12.3 $\mu m^3 \mu m^{-2}$ to 0.43 $\mu m^3 \mu m^{-2}$ as solute travel time increased from 0.6 min to 8.7 min. Total biomass of mixed biofilms also showed a significant inverse relationship over the same range of solute travel time, with observed total biomass decreasing from 27.3 $\mu m^3 \mu m^{-2}$ to 1.27 $\mu m^3 \mu m^{-2}$.

We will now consider the inverse relationship between biofilm biomass and travel time for the mixed culture in more detail. Under the fast inflow condition, regions R2 and R4 had similar velocities and shear stresses, but biomass abundance in R2 was 19.1 $\mu m^3 \mu m^{-2}$, greater than that observed at R4 (17.0 $\mu m^3 \mu m^{-2}$). This difference is explained by the difference in the solute travel time to these regions. The travel time to R2 was much faster than to R4 (1.1 min vs. 1.8 min). Regions R3, R5 and R7 also showed similar local velocities but inverse relationships between travel time and biomass (travel times: R3 = 0.8 min, R5 = 1.3 min, R7 = 2.1 min, biomass accumulation: R3 = 20.6 $\mu m^3 \mu m^{-2}$, R5 =19.7 $\mu m^3 \mu m^{-2}$ and R7 = 15.8 $\mu m^3 \mu m^{-2}$). The only exception to this trend was region R8 under the fast flow condition, where the travel time was 1.1 min but the accumulated biomass was 29.4 $\mu m^3 \mu m^{-2}$. No clear relationship was found between biomass accumulation and solute travel distance in either single- or mixed-species biofilms under either flow condition (Supplementary Figure 1). Note that the fluid velocity varies substantially within the flow cell (Figure 1), so the solute travel time is not linearly proportional to the solute travel distance. Therefore, these results indicate that the travel time, and not simply travel distance,

provides the best measure of the consumption of growth medium from community metabolism along flow paths.

4 Discussion

We studied interactions between *Pseudomonas* and *Flavobacterium* in mixed-species biofilms under imposed flow gradients to evaluate relationships between environmental conditions, community structure (dominant organism), and biofilm morphology. We found that *Pseudomonas* and *Flavobacterium* showed different behavior in single- and mixed-species biofilms due to interactions between the two organisms. Further, the interactions between the two organisms varied between competitive and synergistic depending on external flow conditions.

Competitive interactions occurred under slow-flow conditions, which provide a lower supply of growth medium, including nutrients and substrates that support biomass synthesis and substrates that support catabolism. The delivery of nutrients and substrates to cells involves not only bulk transport into and through the flow cell, but also transport from the bulk fluid into and through the biofilm. Mathematical simulations and experimental results have shown that faster bulk fluid flow increases the delivery of nutrients and substrates into biofilms even under identical bulk influent concentration (Duddu*, et al.*, 2009, Zhang*, et al.*, 2011). Conversely, nutrients and substrates become depleted by cumulative metabolism along flow paths, leading to spatial patterns in biofilm development. We observed a positive correlation between biomass abundance and influx of growth medium, and a negative correlation between biomass abundance and solute travel time, suggesting that biofilm growth was limited by progressive depletion of nutrients and/or substrates along flow paths within the flow cell. Under competitive conditions, with nutritional limitations imposed by slow influx of growth medium, *Pseudomonas* accumulated less biomass in mixed biofilms than in single-species culture. Moreover, the spatial distributions of *Pseudomonas* and *Flavobacterium* also reflected their competition for growth medium in mixed biofilms. *Flavobacterium* secured greater opportunity for nutrient replenishment by colonizing the top layer of the biofilm and generating greater surface area. *Pseudomonas* was overgrown by *Flavobacterium* and was therefore restricted to the poorer nutritional environment at the base of the biofilm. Similar spatial structure had been observed previously in co-culture of *P. aeruginosa* and *Agrobacterium tumefaciens*, but in that consortium *P. aeruginosa* predominated and buried *A. tumefaciens* (An*, et al.*, 2006). Here, the specific growth rate of *Flavobacterium* under the experimental temperature (25°C) was greater than that of *Pseudomonas*, suggesting that *Flavobacterium* was able to win the competition for access to fresh growth medium in the mixed biofilm simply by out-growing, and ultimately over-growing *Pseudomonas*. Liu *et al.* (2009) similarly found that trends in growth rate observed in batch do not always hold in more complex open systems. The absence of sensitivity to metabolic products from either organism suggests that metabolic inhibition did not influence growth patterns, but rather simple competition for resources caused the decreased growth of *Pseudomonas* in mixed biofilms under slow inflow conditions. Thus, *Flavobacterium* won the competition for nutrients and substrates under slow flow conditions and its existence inhibited the growth of *Pseudomonas* by limiting *Pseudomonas* to poorer-quality habitat.

Different patterns were observed under faster flow conditions that provided increased influx of growth medium. Under the fast-flow conditions, both organisms accumulated significantly more biomass in mixed biofilms than in single-species biofilms, and more biofilm biomass accumulated in regions having higher local velocity. However, single-species biofilms exhibited different behavior. Single-species *Pseudomonas* biofilms accumulated significantly greater biomass under the higher inflow condition, which indicated that increasing influx supported more growth of *Pseudomonas*. We previously

observed a similar positive relationship between fluid velocity and *Pseudomonas* biofilm biomass with Luria-Bertani broth (Zhang*, et al.*, 2011). Higher hydrodynamic shear eventually leads to biofilm detachment (Zhang*, et al.*, 2011), but we didn't observe significant detachment of *Pseudomonas* in the experiments reported here. Conversely, the growth of *Flavobacterium* biofilms in monoculture did not depend on local velocity, and single-species *Flavobacterium* biofilms accumulated less biomass than single-species *Pseudomonas* biofilms. The results indicated that trends of biomass accumulation observed under flow conditions didn't follow growth rates observed in batch experiments. The growth rates observed in mixed-species biofilms also didn't follow trends from single-species biofilms, indicating that spatial patterns of nutrients or substrate depletion substantially modified local growth behavior. In addition, *Flavobacterium* biofilms were more heterogeneous and had more complex surface morphology than *Pseudomonas* biofilms, as evidenced by their greater roughness and surface area. Rougher and more porous morphologies are more easily detached by hydrodynamic shear (Garny*, et al.*, 2008), suggesting that the accumulation of *Flavobacterium* in single-species biofilms was limited by detachment induced by hydrodynamic shear stress. Mixed biofilms showed decreased roughness, which are more stable. Moreover, the competition relationship between *Pseudomonas* and *Flavobacterium* under slow flow rate indicated that they don't produce molecules to help the other. Thus, increased *Flavobacterium* accumulation in mixed-species biofilms can potentially be explained by the changes in the biofilm morphology that occurred in co-culture with *Pseudomonas*.

While we did directly observe local velocities, we expect that biofilm development had a small effect on the flow field in these experiments. R2A medium was used here to be relevant to typical depleted environmental conditions, and only thin biofilms (average thickness < 40 μm) formed in this nutrient-poor environment. Although biofilms have been observed to influence fluid flow patterns (Stoodley*, et al.*, 1994, Manz*, et al.*, 2003), significant changes normally only occur with more extensive biofilm growth. The feedback between biofilm growth and the flow field should be considered when biofilms become thicker. This feedback is likely to be important over the long term and in more nutrient-rich environments.

In sum, our results indicate that inter-species interactions between *Pseudomonas* and *Flavobacterium* in co-cultured biofilms were significantly affected by external flow conditions. While organism-specific growth rates are important in the competition for securing space and providing favorable access to nutrients and substrates, the structural and morphological properties of the biofilm are also important because they mediate both solute delivery to cells within the biofilm and adherence of the community to the surface. We found that biofilm morphology and mechanical properties are particularly important to the accumulation of biomass under flow. This finding suggests that organisms that produce the most resilient biofilms are critical to the colonization of surfaces in flowing waters, as such stable biofilms can provide protected habitat that other organisms can colonize. Similarly, inter-species interactions that favor development of more resilient biofilms can support enhanced colonization of surfaces subject to high hydrodynamic shear. Further, our observation that both species showed greater biomass in mixed biofilms suggests that synergy arises from increased efficiency of overall community metabolism as a result of the spatial segregation of organisms within the biofilm. Such enhanced community metabolism depends not only on the metabolic capability of each organism, but also on the spatial configuration and mechanical properties of the biofilm because these properties determine the regions that can be colonized by each organism in the community. This was exemplified here by the structural changes to the biofilm that allowed *Flavobacterium* to accumulate more biomass in co-culture with *Pseudomonas* than it could on its own. These findings are important because they indicate that the behavior of multi-species biofilms cannot be

understood purely by integrating information obtained from a sense of independent investigations of individual organisms. Instead, it is necessary to specifically identify ecological interactions between species that influence the exploitation of the environment by complex communities.

Supplementary Material

Refer to Web version on PubMed Central for supplementary material.

References

An DD, Danhorn T, Fuqua C, Parsek MR. Quorum sensing and motility mediate interactions between Pseudomonas aeruginosa and Agrobacterium tumefaciens in biofilm cocultures. Proceedings of the National Academy of Sciences of the United States of America. 2006; 103:3828–3833. [PubMed: 16537456]

Anaissie EJ, Penzak SR, Dignani MC. The hospital water supply as a source of nosocomial infections. Archives of Internal Medicine. 2002; 162:1483–1492. [PubMed: 12090885]

Battin TJ, Kaplan LA, Newbold JD, Hansen CME. Contributions of microbial biofilms to ecosystem processes in stream mesocosms. Nature. 2003; 426:439–442. [PubMed: 14647381]

Beaufort S, Da Silva T, Lafforgue C, Alfenore S. Fluorescent proteins as in-vivo and in-situ reporters to study the development of a Saccharomyces cerevisiae yeast biofilm and its invasion by the bacteria Escherichia coli. Fems Microbiology Ecology. 2012; 80:342–351. [PubMed: 22268656]

Brinkmeyer R, Knittel K, Jurgens J, Weyland H, Amann R, Helmke E. Diversity and structure of bacterial communities in arctic versus antarctic pack ice. Applied and Environmental Microbiology. 2003; 69:6610–6619. [PubMed: 14602620]

Chopp DL, Kirisits MJ, Moran B, Parsek MR. A mathematical model of quorum sensing in a growing bacterial biofilm. Journal of Industrial Microbiology & Biotechnology. 2002; 29:339–346. [PubMed: 12483476]

Davey ME, O'toole GA. Microbial biofilms: from ecology to molecular genetics. Microbiology and Molecular Biology Reviews. 2000; 64:847. [PubMed: 11104821]

Duddu R, Chopp DL, Moran B. A Two-Dimensional Continuum Model of Biofilm Growth Incorporating Fluid Flow and Shear Stress Based Detachment. Biotechnology and Bioengineering. 2009; 103:92–104. [PubMed: 19213021]

Elvers KT, Leeming K, Moore CP, Lappin-Scott HM. Bacterial-fungal biofilms in flowing water photo-processing tanks. Journal of Applied Microbiology. 1998; 84:607–618. [PubMed: 9633659]

Ford TE. Microbiological safety of drinking water: United States and global perspectives. Environmental Health Perspectives. 1999; 107:191–206. [PubMed: 10229718]

Garny K, Horn H, Neu TR. Interaction between biofilm development, structure and detachment in rotating annular reactors. Bioprocess and Biosystems Engineering. 2008; 31:619–629. [PubMed: 18320233]

Hansen SK, Rainey PB, Haagensen JAJ, Molin S. Evolution of species interactions in a biofilm community. Nature. 2007; 445:533–536. [PubMed: 17268468]

Heydorn A, Ersboll BK, Hentzer M, Parsek MR, Givskov M, Molin S. Experimental reproducibility in flow-chamber biofilms. Microbiology-Uk. 2000; 146:2409–2415.

Heydorn A, Nielsen AT, Hentzer M, Sternberg C, Givskov M, Ersboll BK, Molin S. Quantification of biofilm structures by the novel computer program COMSTAT. Microbiology-Uk. 2000; 146:2395–2407.

Kolenbrander PE. Oral microbial communities: Biofilms, interactions, and genetic systems. Annual Review of Microbiology. 2000; 54:413–437.

Liu Y, Tay JH. The essential role of hydrodynamic shear force in the formation of biofilm and granular sludge. Water Research. 2002; 36:1653–1665. [PubMed: 12044065]

Liu Y, Zhang W, Sileika T, Warta R, Cianciotto NP, Packman A. Role of bacterial adhesion in the microbial ecology of biofilms in cooling tower systems. Biofouling. 2009; 25:241–253. [PubMed: 19177226]

Liu Y, Zhang W, Sileika T, Warta R, Cianciotto NP, Packman AI. Disinfection of bacterial biofilms in pilot-scale cooling tower systems. Biofouling. 2011; 27:393–402. [PubMed: 21547755]

Manz B, Volke F, Goll D, Horn H. Measuring local flow velocities and biofilm structure in biofilm systems with magnetic resonance imaging (MRI). Biotechnology and Bioengineering. 2003; 84:424–432. [PubMed: 14574699]

Manz W, Wendt-Potthoff K, Neu TR, Szewzyk U, Lawrence JR. Phylogenetic composition, spatial structure, and dynamics of lotic bacterial biofilms investigated by fluorescent in situ hybridization and confocal laser scanning microscopy. Microbial Ecology. 1999; 37:225–237. [PubMed: 10341052]

Murga R, Forster TS, Brown E, Pruckler JM, Fields BS, Donlan RM. Role of biofilms in the survival of Legionella pneumophila in a model potable-water system. Microbiology-Sgm. 2001; 147:3121–3126.

Nikoskelainen S, Salminen S, Bylund G, Ouwehand AC. Characterization of the properties of human- and dairy-derived probiotics for prevention of infectious diseases in fish. Applied and Environmental Microbiology. 2001; 67:2430–2435. [PubMed: 11375147]

Orrison LH, Bibb WF, Cherry WB, Thacker L. Determination of Antigenic Relationships among Legionellae and Non-Legionellae by Direct Fluorescent-Antibody and Immunodiffusion Tests. Journal of Clinical Microbiology. 1983; 17:332–337. [PubMed: 6403577]

Overmann J, van Gemerden H. Microbial interactions involving sulfur bacteria: implications for the ecology and evolution of bacterial communities. Fems Microbiology Reviews. 2000; 24:591–599. [PubMed: 11077152]

Pearson ML, Farr BM, Garland JS, Mermel LA, Raad II, Sheretz RJ, Stover BH. Guideline for prevention of intravascular device-related infections.1. Intravascular device-related infections: An overview. American Journal of Infection Control. 1996; 24:262–293. [PubMed: 8870910]

Purevdorj B, Costerton JW, Stoodley P. Influence of hydrodynamics and cell signaling on the structure and behavior of Pseudomonas aeruginosa biofilms. Applied and Environmental Microbiology. 2002; 68:4457–4464. [PubMed: 12200300]

Sekiguchi Y, Kamagata Y, Nakamura K, Ohashi A, Harada H. Fluorescence in situ hybridization using 16S rRNA-targeted oligonucleotides reveals localization of methanogens and selected uncultured bacteria in mesophilic and thermophilic sludge granules. Applied and Environmental Microbiology. 1999; 65:1280–1288. [PubMed: 10049894]

Stamm WE, Colella JJ, Anderson RL, Dixon RE. Indwelling Arterial Catheters as a Source of Nosocomial Bacteremia - Outbreak Caused by Flavobacterium Species. New England Journal of Medicine. 1975; 292:1099–1102. [PubMed: 1128554]

Stoodley P, Debeer D, Lewandowski Z. Liquid Flow in Biofilm Systems. Applied and Environmental Microbiology. 1994; 60:2711–2716. [PubMed: 16349345]

Stover CK, Pham XQ, Erwin AL, et al. Complete genome sequence of Pseudomonas aeruginosa PAO1, an opportunistic pathogen. Nature. 2000; 406:959–964. [PubMed: 10984043]

Ward DM, Ferris MJ, Nold SC, Bateson MM. A natural view of microbial biodiversity within hot spring cyanobacterial mat communities. Microbiology and Molecular Biology Reviews. 1998; 62:1353. [PubMed: 9841675]

Zengler K. Central Role of the Cell in Microbial Ecology. Microbiology and Molecular Biology Reviews. 2009; 73:712–729. [PubMed: 19946138]

Zhang W, Sileika TS, Chen C, Liu Y, Lee J, Packman AI. A novel planar flow cell for studies of biofilm heterogeneity and flow-biofilm interactions. Biotechnology and Bioengineering. 2011; 108:2571–2582. [PubMed: 21656713]

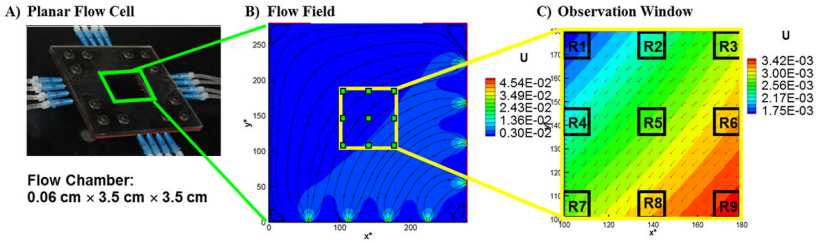

Figure 1.

A) Photograph of the planar flow cell. B) The flow field in the flow chamber with streamlines under inflow rate of 0.16 mL min^{-1}. C) The observation window in the center of the flow chamber, including locations of nine regions observed by confocal microscopy. Coordinates are lattice locations normalized by lattice spacing (Zhang*, et al.*, 2011), and color bars of U represent lattice dimensionless fluid velocity increased from blue to red.

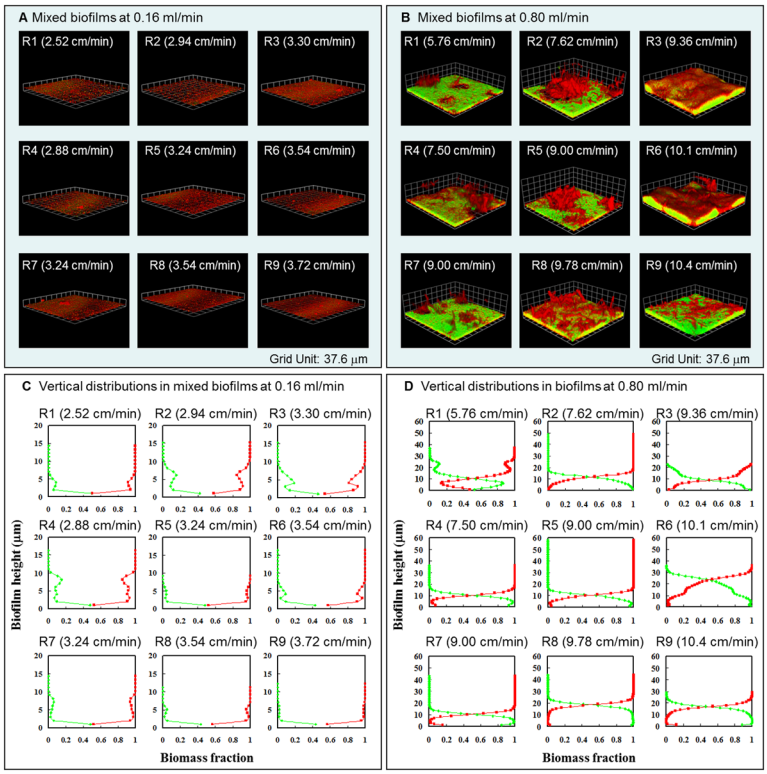

Figure 2.

Dual-species seven-day-old biofilms of *Pseudomonas aeruginosa* PAO1 (green) and *Flavobacterium sp.* CDC-65 (red) under inflow rates of 0.16 mL min^{-1} and 0.8 mL min^{-1}. A) and B) show the representative biofilm morphology on the 7^{th} day at each of the nine regions indicated in Figure 1C. Local velocities in each region are given in parentheses, and the grid unit is 37.6 μm. C) and D) show the representative vertical distributions of *Pseudomonas* and *Flavobacterium* at each region of the biofilm. Red lines represent the fraction of *Flavobacterium* and green lines represent the fraction of *Pseudomonas*.

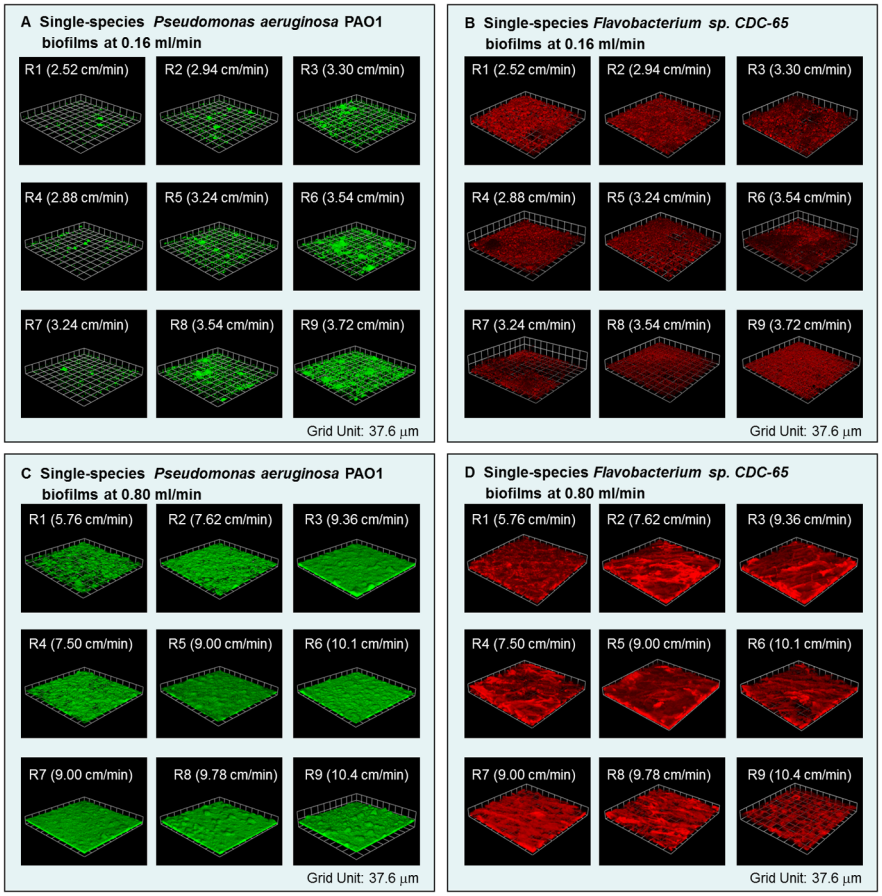

Figure 3.

Representative seven-day-old single-species biofilms of *Pseudomonas aeruginosa* PAO1 and *Flavobacterium sp.* CDC-65 under inflow rates 0.16 mL min^{-1} and 0.80 mL min^{-1}. Results are shown for each of the nine regions indicated in Figure 1C. Local velocities in each region are given in parentheses, and the grid unit is 37.6 μm.

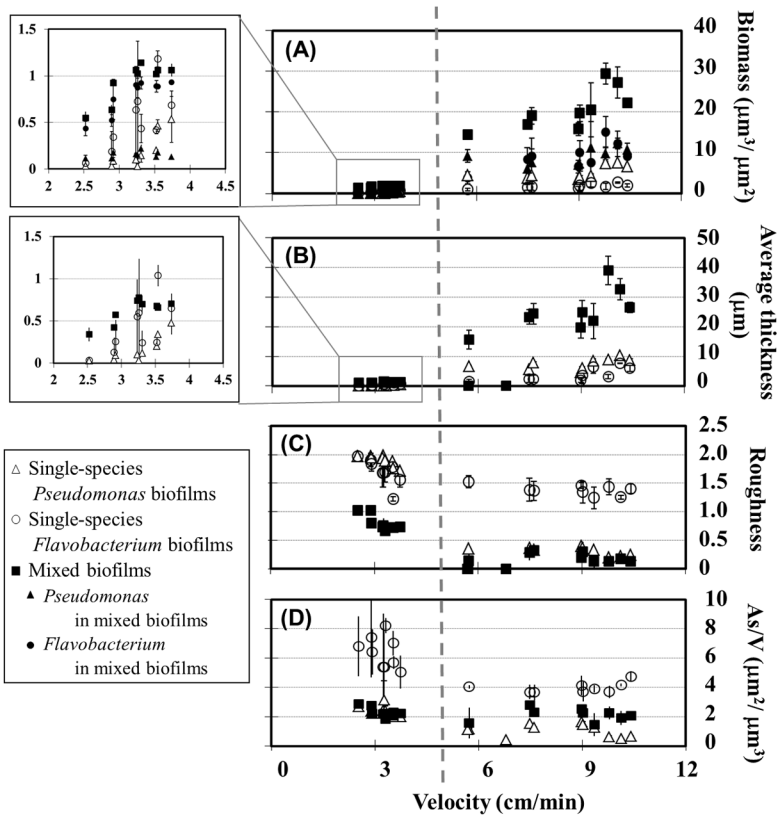

Figure 4.

Biofilm biomass and morphology as a function of local velocity in single- and mixed-species biofilms. Open symbols represent single-species biofilms of *Pseudomonas aeruginosa* PAO1 and *Flavobacterium sp.* CDC-65, and solid symbols represent mixed biofilms. A) Total biomass of single- and mixed-species biofilms, and biomass of each organism within mixed biofilms. B) Average thickness, C) Roughness and D) Surface-area-to-volume ratio (As/V) of single- and mixed-species biofilms. Plotted points and error bars represent the average and standard deviation of three replicate observations. Similar trends were observed in other experiments.

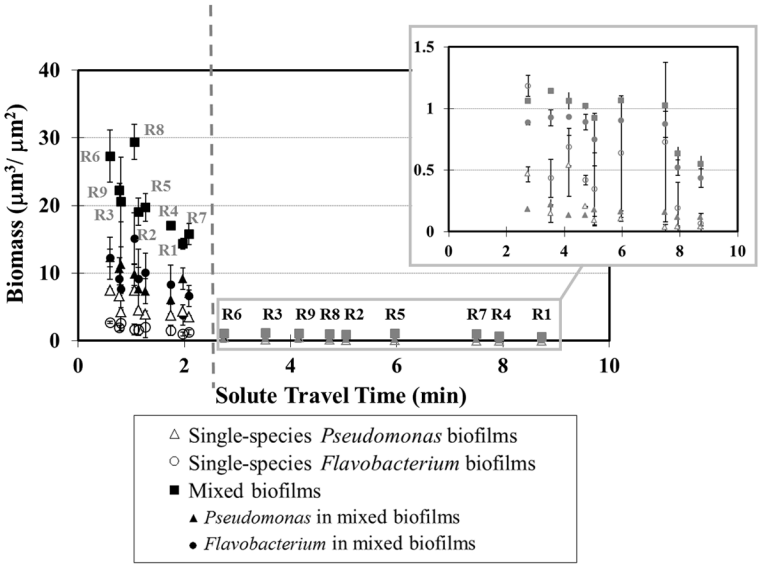

Figure 5.

Relationship between biofilm biomass and solute travel time from the flow-cell inlet to the observation locations. Open symbols represent single-species biofilms, and solid symbols represent mixed biofilms. Black icons show observations obtained under fast inflow rate (0.80 mL min^{-1}), and gray icons in the inset show observations obtained under the slow inflow rate (0.16 mL min^{-1}). Plotted points and error bars represent the average and standard deviation of three replicate observations. Similar trends were observed in other experiments.